RESEARCH IN SUPERCRITICAL FUEL PROPERTIES AND COMBUSTION MODELING

Gregory Faris
SRI INTERNATIONAL MENLO PARK CA

09/18/2015
Final Report

REPORT DOCUMENTATION PAGE

Form Approved
OMB No. 0704-0188

Public reporting burden for this collection of information is estimated to average 1 hour per response, including the time for reviewing instructions, searching existing data sources, gathering and maintaining the data needed, and completing and reviewing this collection of information. Send comments regarding this burden estimate or any other aspect of this collection of information, including suggestions for reducing this burden to Department of Defense, Washington Headquarters Services, Directorate for Information Operations and Reports (0704-0188), 1215 Jefferson Davis Highway, Suite 1204, Arlington, VA 22202-4302. Respondents should be aware that notwithstanding any other provision of law, no person shall be subject to any penalty for failing to comply with a collection of information if it does not display a currently valid OMB control number. **PLEASE DO NOT RETURN YOUR FORM TO THE ABOVE ADDRESS.**

1. REPORT DATE *(DD-MM-YYYY)*	2. REPORT TYPE	3. DATES COVERED *(From - To)*
14-09-2015	Final Technical Report	15-June-2013 – 14-June-2015

4. TITLE AND SUBTITLE
Research in Supercritical Fuel Properties and Combustion Modeling

5a. CONTRACT NUMBER

5b. GRANT NUMBER
FA9550-13-1-0177

5c. PROGRAM ELEMENT NUMBER

6. AUTHOR(S)
Gregory W. Faris, Gregory P. Smith

5d. PROJECT NUMBER

5e. TASK NUMBER

5f. WORK UNIT NUMBER

7. PERFORMING ORGANIZATION NAME(S) AND ADDRESS(ES)

SRI International
333 Ravenswood Avenue
Menlo Park, CA 94025-3493

8. PERFORMING ORGANIZATION REPORT NUMBER

9. SPONSORING / MONITORING AGENCY NAME(S) AND ADDRESS(ES)
AFOSR/NA
875 Randolph Street
Suite 325, Room 3112
Arlington, VA 22203

10. SPONSOR/MONITOR'S ACRONYM(S)

11. SPONSOR/MONITOR'S REPORT NUMBER(S)

12. DISTRIBUTION / AVAILABILITY STATEMENT

Approved for public release; distribution unlimited

13. SUPPLEMENTARY NOTES

14. ABSTRACT

The objectives of this research are to develop stimulated scattering as a diagnostic for supercritical fluids, and to evaluate reaction kinetics inputs involving 2-4 carbon atom species for combustion modeling and optimization. On the stimulated scattering task, we have tested new methods for rapidly scanning stimulated scattering measurements, achieving a factor of 1,000 improvement in the single shot spectroscopy measurement rate; developed models for two-tone stimulated Rayleigh scattering signals; published a paper on our new two-tone stimulated scattering method, implemented frequency domain measurements for refractive index measurements, and tested our supercritical cell. On the reaction kinetics task, review and evaluation of reactions, rate parameters, and uncertainties for combustion of 2-carbon species for the initial foundational fuels mechanism optimization was completed. We identified reactions needing further study and C-2 and C-3 species to add to the mechanism.

15. SUBJECT TERMS
Supercritical fluids, Brillouin scattering, Rayleigh scattering, elastic properties, thermal properties; combustion chemistry, ethylene, reaction rate parameters

16. SECURITY CLASSIFICATION OF:			17. LIMITATION OF ABSTRACT	18. NUMBER OF PAGES	19a. NAME OF RESPONSIBLE PERSON
a. REPORT	**b. ABSTRACT**	**c. THIS PAGE**	UL	19	Chiping Li
Unclassified	Unclassified	Unclassified			**19b. TELEPHONE NUMBER** *(include area code)* (703) 696-8574

Standard Form 298 (Rev. 8-98)
Prescribed by ANSI Std. Z39.18

DISTRIBUTION A: Distribution approved for public release.

SRI International

Final Technical Report • September 14, 2015

RESEARCH IN SUPERCRITICAL FUEL PROPERTIES AND COMBUSTION MODELING

Prepared by:

Gregory W. Faris, Gregory P. Smith

SRI Project 21929
Grant Number FA9550-13-1-0177

Prepared for:

Air Force Office of Scientific Research
AFOSR/NA
875 Randolph Street
Suite 325, Room 3112
Arlington VA 22203

Attn: Dr. Chiping Li

REPORT DOCUMENTATION PAGE

Form Approved
OMB No. 0704-0188

Public reporting burden for this collection of information is estimated to average 1 hour per response, including the time for reviewing instructions, searching existing data sources, gathering and maintaining the data needed, and completing and reviewing this collection of information. Send comments regarding this burden estimate or any other aspect of this collection of information, including suggestions for reducing this burden to Department of Defense, Washington Headquarters Services, Directorate for Information Operations and Reports (0704-0188), 1215 Jefferson Davis Highway, Suite 1204, Arlington, VA 22202-4302. Respondents should be aware that notwithstanding any other provision of law, no person shall be subject to any penalty for failing to comply with a collection of information if it does not display a currently valid OMB control number. **PLEASE DO NOT RETURN YOUR FORM TO THE ABOVE ADDRESS.**

1. REPORT DATE (DD-MM-YYYY)	2. REPORT TYPE	3. DATES COVERED (From - To)
14-09-2015	Final Technical Report	15-June-2013 – 14-June-2015

4. TITLE AND SUBTITLE
Research in Supercritical Fuel Properties and Combustion Modeling

5a. CONTRACT NUMBER

5b. GRANT NUMBER
FA9550-13-1-0177

5c. PROGRAM ELEMENT NUMBER

6. AUTHOR(S)
Gregory W. Faris, Gregory P. Smith

5d. PROJECT NUMBER

5e. TASK NUMBER

5f. WORK UNIT NUMBER

7. PERFORMING ORGANIZATION NAME(S) AND ADDRESS(ES)

SRI International
333 Ravenswood Avenue
Menlo Park, CA 94025-3493

8. PERFORMING ORGANIZATION REPORT NUMBER

9. SPONSORING / MONITORING AGENCY NAME(S) AND ADDRESS(ES)
AFOSR/NA
875 Randolph Street
Suite 325, Room 3112
Arlington, VA 22203

10. SPONSOR/MONITOR'S ACRONYM(S)

11. SPONSOR/MONITOR'S REPORT NUMBER(S)

12. DISTRIBUTION / AVAILABILITY STATEMENT

Approved for public release; distribution unlimited

13. SUPPLEMENTARY NOTES

14. ABSTRACT

The objectives of this research are to develop stimulated scattering as a diagnostic for supercritical fluids, and to evaluate reaction kinetics inputs involving 2-4 carbon atom species for combustion modeling and optimization. On the stimulated scattering task, we have tested new methods for rapidly scanning stimulated scattering measurements, achieving a factor of 1,000 improvement in the single shot spectroscopy measurement rate; developed models for two-tone stimulated Rayleigh scattering signals; published a paper on our new two-tone stimulated scattering method, implemented frequency domain measurements for refractive index measurements, and tested our supercritical cell. On the reaction kinetics task, review and evaluation of reactions, rate parameters, and uncertainties for combustion of 2-carbon species for the initial foundational fuels mechanism optimization was completed. We identified reactions needing further study and C-2 and C-3 species to add to the mechanism.

15. SUBJECT TERMS
Supercritical fluids, Brillouin scattering, Rayleigh scattering, elastic properties, thermal properties; combustion chemistry, ethylene, reaction rate parameters

16. SECURITY CLASSIFICATION OF:			17. LIMITATION OF ABSTRACT	18. NUMBER OF PAGES	19a. NAME OF RESPONSIBLE PERSON Chiping Li
a. REPORT	**b. ABSTRACT**	**c. THIS PAGE**	UL	19	**19b. TELEPHONE NUMBER** (include area code)
Unclassified	Unclassified	Unclassified			(703) 696-8574

Standard Form 298 (Rev. 8-98)
Prescribed by ANSI Std. Z39.18

ABSTRACT

The objectives of this research are to develop stimulated scattering as a diagnostic for supercritical fluids, and to evaluate reaction kinetics inputs involving 2-4 carbon atom species for combustion modeling and optimization. On the stimulated scattering task, we have tested new methods for rapidly scanning stimulated scattering measurements, achieving a factor of 1,000 improvement in the single shot spectroscopy measurement rate; developed models for two-tone stimulated Rayleigh scattering signals; published a paper on our new two-tone stimulated scattering method, implemented frequency domain measurements for refractive index measurements, and tested our supercritical cell. On the reaction kinetics task, review and evaluation of reactions, rate parameters, and uncertainties for combustion of 2-carbon species for the initial foundational fuels mechanism optimization was completed. We identified reactions needing further study and C-2 and C-3 species to add to the mechanism.

OBJECTIVES

The objectives of this research are to develop stimulated scattering as a diagnostic for supercritical fluids, and to evaluate reaction kinetics inputs involving 2-4 carbon atom species for combustion modeling and optimization. The goals of this research are:

- Making improvements on our optical stimulated scattering method to enable rapid measurement of stimulated Brillouin scattering.
- Combining the stimulated scattering measurements with in-situ refractive index measurements to convert spectroscopic properties to physical properties.
- Comparing measured properties on single component hydrocarbons with the NIST REFPROP database in the supercritical regime.
- Performing measurements on jet fuel under supercritical conditions.
- Developing an evaluated and optimized combustion kinetics model for unsaturated and other hydrocarbon fuels containing up to 2 carbon atoms.
- Updating and expanding this model with additional kinetics and optimization targets to accommodate unsaturated $C_{3-4}H_X$ fuel fragments.

RESULTS OF EFFORT

STIMULATED SCATTERING

- We have tested new methods for rapidly scanning stimulated scattering measurements, achieving a factor of 1,000 improvement in the single shot spectroscopy measurement rate.
- We have developed models for two-tone stimulated Rayleigh scattering signals.
- We have published a paper on two-tone stimulated scattering.
- We have developed a frequency domain system for the refractive index measurement required to convert stimulated Rayleigh/Brillouin scattering measurements to thermal and viscoelastic properties.
- We have tested our high pressure high temperature cell to 4800 psi and 600 C.

REACTION KINETICS

- We developed and evaluated a pressure and temperature dependent kinetics mechanism for combustion of hydrocarbon fuels containing up to 2 carbon atoms, including uncertainties.
- We identified key reactions and additional species for mechanism refinement, including additions for 3 carbon species oxidation.

ACCOMPLISHMENTS / NEW FINDINGS

STIMULATED SCATTERING DIAGNOSTICS

Instrumentation and Methods

We have demonstrated the two-tone frequency modulation stimulated Rayleigh spectroscopy method.[1] This method combines high spectral resolution (~1 MHz), excellent pump-probe detuning accuracy, and near-shot-noise limited signal-to-noise ratios. These are all important properties for the measurement of supercritical fuel properties. Our prior studies have shown that the stimulated Rayleigh linewidths become very narrow in the supercritical regime, preventing use of conventional Q-switched laser systems and separate pump and probe laser sources.[2] Our new instrumentation meets the needs in the supercritical regime. The two-tone method derives both pump and probe beams from a single laser source, with the tuning provided by electrooptical modulation. Pulse amplification of the pump laser allows much narrower linewidths than the Q-switched laser.

We are the first to perform two-tone stimulated scattering. The phase dependence of the two-tone signal showed unusual behavior with the antisymmetric (gain/loss) features having the same sign for the two sidebands, while the symmetric (phase change) features are opposite in sign (Figure 1). We have examined the theory for the two-tone signal and derived the new expression for the sample gain/loss and phase as described by $\exp(-\delta_j - i\phi_j)$

$$-\left(\delta_{+1} + \delta_{-1}\right)\cos\left(\Omega t\right) - \left(\phi_{+1} - \phi_{-1}\right)\sin\left(\Omega t\right)$$

where Ω is the two-tone frequency pair separation frequency and $j = +1$ and -1 denote the upper and lower sidebands, respectively. This behavior is in agreement with that observed in Figure 1.
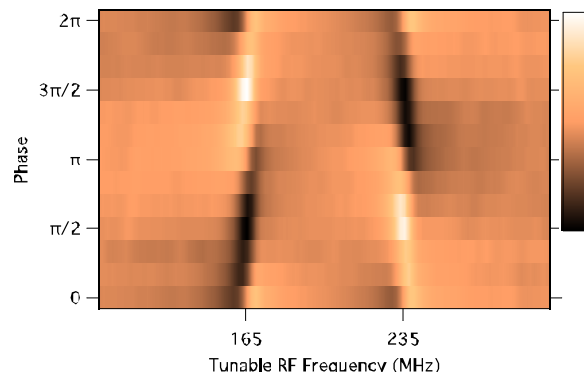

Figure. 1. Variation in experimental two-tone FM stimulated Rayleigh spectra in hexane as a function of delay between probe and reference signal to the I/Q demodulator.

With electrooptic modulation, we have shown that the two-tone method can provide a very rapid sweep over a scattering peak in a single laser shot at a repetition rate of 10 Hz. With support from a National Science Foundation Major Research Instrumentation grant, we have been able to upgrade our instrumentation for these measurements. The new instrumentation includes a higher power probe laser and a continuous-wave pumped amplifier for the pump beam. Using this apparatus, we have been able to acquire single-shot spectra at a repetition rate of 10,000 spectra per second, an increase by a factor of 1,000 over our previous result. Single shot acquisition will enhance our ability to obtain accurate property measurements in supercritical fuels by avoiding the problems associated with intensity fluctuations produced by fluid fluctuations when performing a spectral scan using many point measurements from a pulsed laser. The high spectra acquisition rate is essential for monitoring fluctuations known to exist in supercritical fluids.

Frequency Domain Refractive Index Measurement

Refractive index measurements are required to convert the stimulated Rayleigh/Brillouin spectroscopic measurements to thermal and viscoelastic properties for supercritical fuels. We are applying frequency domain measurements to the measurements of refractive index. This approach works well for measurements in a supercritical cell for a number of reasons. First, we can perform the measurements at the same wavelength as the stimulated scattering measurements, which is ideal since the refractive index varies with wavelength. Second, the method only requires that a laser beam pass through the cell, so that it can be performed even when optical access is limited as is the case for high pressure, high temperature cells. Finally, although the signals are periodic in refractive index, the period is well-matched the measurement requirements. This is in contrast with conventional interferometry, for which the period of the signal (one fringe) occurs for an optical pathlength change of a half wavelength. This is far too sensitive for practical use in a high pressure, high temperature cell, in which case the enormous number of fringes in the cell leads to difficulty counting fringes and makes it easy to lose count. For frequency domain measurements, the light is amplitude modulated and the phase of the amplitude modulation is measured rather than the phase of the light itself. We use a modulation frequency of ~480 MHz. This leads to a modulation wavelength in the cell of ~4 cm. Thus it is

5

impossible to lose count of the modulation phase. Using the improvements described below, we can measure phase with frequency domain measurements to approximately 0.1 degree. This leads to an uncertainty in the refractive index of less than 1%, which is more than adequate for the required property measurements.

The apparatus we have developed for frequency domain refractive index measurements is shown in Figure 2. Photographs of the apparatus are shown in Figures 3 and 4. A number of modifications were required to achieve good phase stability, which is what determines the refractive index accuracy. Frequency domain measurements are susceptible to interference from both optical and electrical background at the measurement frequency.[3] Both types of interference can produce phase drift or systematic phase offsets that degrade the accuracy of the measurements. We have performed careful studies of the influence of these backgrounds using both homodyne and heterodyne measurements. For the heterodyne measurements, the two phase-locked frequencies were provided using two channels from an arbitrary waveform generator. We found that the dominant source of background was RF pickup at the input to an amplifier driving the laser diode. Placing the laser diode and amplifier in an aluminum box shielded this background quite effectively.
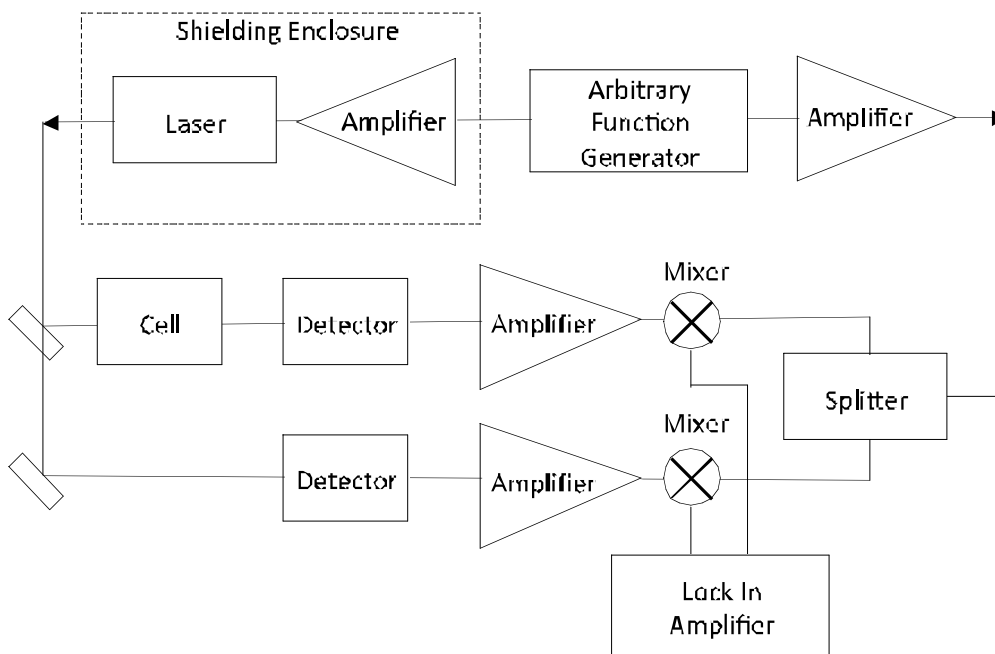

Figure 2. New apparatus for frequency domain refractive index measurements.

Another systematic source of error proved to be phase drift between the electrical signal to the laser diode and the light emitted by the fiber pigtail of the laser. This may be related to temperature changes in the laser diode output and phase drift or phase-motion sensitivity in the fiber pigtail. We found that waiting for the laser to warm up reduced this drift, but it was still too large. To eliminate this drift, we are using the laser diode to provide the reference frequency. This configuration requires that the signal and reference frequencies are the same. We are performing heterodyne mixing to convert these two signals to lower frequency.

With a laser reference source, we require two detectors, one for the reference beam and one for the measurement or signal beam. We had planned to use 80 to 100 micron diameter photodiodes for this purpose, which offer ample bandwidth for the 480 MHz signal, but the small

detector diameter makes light collection more difficult. We found that combining low capacitance 0.5 mm InGaAs photodiodes with low input impedance transimpedance amplifiers we were able to get good response beyond 500 MHz. This provides a factor of 25 to 40 times larger detection area compared with the smaller photodiodes.

With the optical reference method, we found one additional source of background interference. We use two frequencies for the optical reference method, one for the laser diode and a second as a heterodyne. The detector signal and heterodyne signal are combined in RF mixers to bring the frequencies down to lower frequencies for lock-in detection. We found that there was RF crosstalk between the two channels because of the common circuitry used to split the RF reference signal. We were able to bring this crosstalk down to acceptable levels by placing amplifiers and attenuators between the RF reference splitter and the mixers.

Figure 3. Photograph of electronics for frequency domain measurements showing box containing laser diode and amplifier (top), laser diode current and temperature controllers (middle), and lock-in amplifier (bottom).
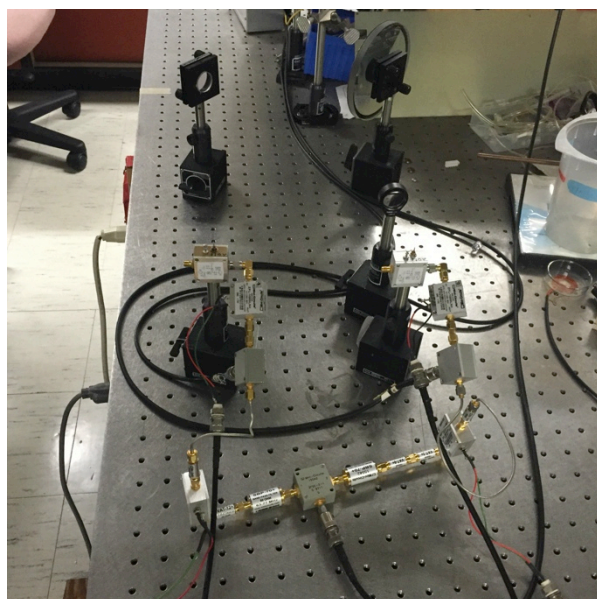

Figure 4. Photograph of optics for frequency domain measurements showing fiber source, beam splitter, detectors, and RF electronics.

Supercritical Cell

In preparation for new supercritical measurements, we have tested our cell at high pressures and temperatures. Although we desire operation to 1500 psi and 600 C, the cell is to be tested to 4 times the pressure to meet safety requirements. While the operating pressure and temperature are achievable, getting the cell to a test condition of 6000 psi at 600 C proved very challenging. The only seal type that can operate at these high temperatures and pressures is graphite, and 6000 psi and 600 C is very high for even graphite.

A photograph of the cell with the window configure indicated is in Figure 5. A diagram and photographs of the test setup are shown in Figures 6 and 7, respectively. For testing we used nitrogen gas. An ultrahigh pressure (6,000 psi) nitrogen cylinder with regulator was used as the pressure source. An Omega PX309-10KG5V pressure transducer was used to measure the pressure. A Cole-Parmer 89000-10 temperature controller controlled the heater. A secondary

thermometer was installed for the additional reference. Both temperature and pressure were monitored by a laptop. The setup was located in a high pressure containment cell at SRI.

We tried a number of conditions to reach the full test conditions. The windows were tightened with cone washers under the nuts to maintain pressure on the seals during thermal expansion. Cone washers were stacked either in one direction to maximize the force or in opposite directions to maximize the potential deflection. With lower torque on the nuts, the graphite seals failed. At higher torque, the windows cracked. The cracks did not form immediately, but formed as long as a day later. We tried using very thin graphite seals on the hypothesis that there would be a smaller area subject to the pressure with the same surface contact to support the seal. This did not help achieve the higher pressures. To achieve a testable pressure, we replaced the windows with steel windows only for the purpose of the test. With this configuration, we were able to reach 4800 psi and 600 C. This test confirms that the cell itself can withstand the required pressures. If the windows fail, they will be contained with a Lexan box.
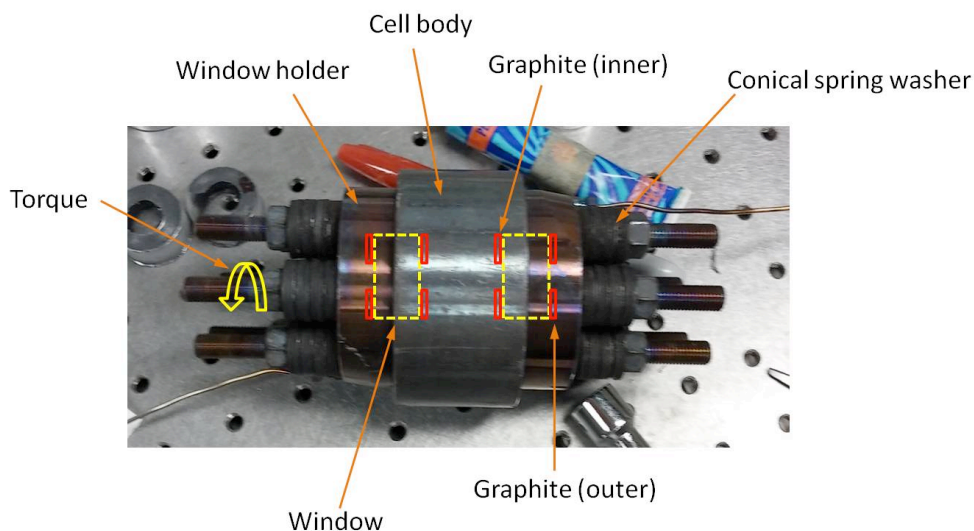

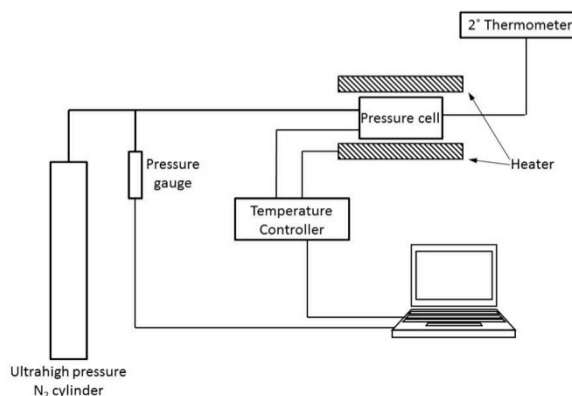Figure 5. High pressure cell configuration.

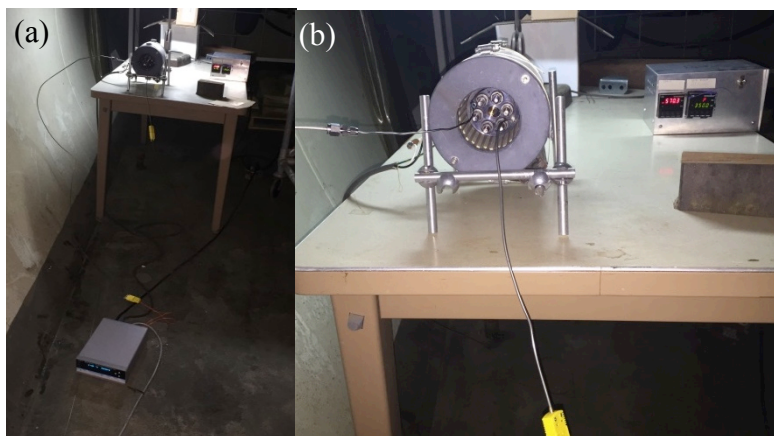Figure 6. Test set up for high pressure cell.

Figure 7.(a) shows the presure cell/heater, temperature controller and thermocouple; (b) an enlarged view of presure cell/heater and thermocouple.

REACTION KINETICS

The development of accurate and reliable chemical mechanisms and models to predict the combustion behavior of jet fuel surrogates and compounds (petroleum, synthetic, and biological), is an important Air Force goal relevant to maintaining aircraft performance and safety. The chemical mechanisms for combustion of all of these fuels share the same set of elementary reactions of smaller-fragment hydrocarbons, and thus a reliable submodel accurately describing the pyrolysis and oxidation kinetics of small species, both hydrocarbons and partially oxygenated intermediates, is critical to these efforts. In fact, for most complex fuels and mixtures under combustion conditions, the initial decomposition into smaller fragments is fast, and the models are sensitive to the product identities and the shared small fragment chemistry. SRI has worked with Prof. Hai Wang (Stanford) and DOE-CEFRC- and AFOSR-sponsored colleagues to begin development of an evaluated and optimized foundational fuels mechanism for this base chemistry. Acknowledgements are due to Prof. Wang, Dr. Enoch Dames, Ms. Yujie Tao for their assistance in this effort, as well as to many colleagues engaged in similar efforts recorded in the literature. Optimization of the initial evaluated C1-2 mechanism is near completion, considering 45 reactive species and 450 reactions. (For a discussion of the optimization philosophy and procedure, which is designed to accurately model basic combustion property target experiments while being consistent with known kinetics values see references 4, 5, and citations therein). A full and quite lengthy listing of the base and optimized mechanisms with source information for the rate constant parameters will be prepared and made available to the community, with proper acknowledgement, via the Internet, when the mechanism optimization calculations are completed and validated. Some important kinetics issues raised in the rate constant evaluation effort are summarized below. This is an ongoing effort, revised as new information on key reactions becomes available. Obviously the optimization target modeling reaction sensitivities and their uncertainties guide which reactions merit further attention, some of which are mentioned below.

To ensure consistency and accuracy, the complex fuels combustion models should share the same H_2/CO/C1-4 pyrolysis and oxidation submodel, optimized to available experimental combustion data for these smaller fuels. This submodel development begins with a critical evaluation of reaction steps and rate parameter expressions to choose the most reliable and

9

consistent values (over suitable temperature and pressure ranges), and to ascertain uncertainties. These judged uncertainties, often hard to fix precisely, determine how much key rate constant parameters will be permitted to vary in the mechanism optimization procedure.

In the course of evaluating the reactions and pressure and temperature dependent rate parameters for the oxidation chemistry of two-carbon fuels, several specific revision needs were identified. These will be incorporated into the second optimized foundational fuels mechanism. Several are of particular importance due to the prevalence of ethylene as a major breakdown intermediate of larger real fuel mixtures.

Two stable isomers of CH_3CHO are not included in the current mechanism and needed to be added, namely vinyl alcohol and ethylene oxide (oxirane), C_2H_3OH and cy-C_2H_4O. C_2H_4O kinetics in particular have a significant effect on ethylene ignition, via the $HO_2 + C_2H_4$ production reaction and then subsequent C_2H_4O decomposition to $CH_3 + HCO$, which is highly chain branching. (Production of extra radicals accelerates the chemistry.) Inclusion should remedy a significant omission. In considering vinyl alcohol, the $OH + C_2H_3$ chemical activation reactions which have received little attention were also reevaluated. Faster rate constants to the $CH_3 + HCO$ and $H + CH_2CHO$ products are indicated. A few extra HO_2 reactions were also added for mechanism completeness, especially $HO_2 + C_2H_X$.

Ethylene decomposition in the current mechanism is very poorly parameterized, the result of an attempt to account for in-progress Stanford data,[6] with limited success. Rates under many conditions are, we believe, too fast in the 1.0 base mechanism. There are issues of both experimental and theoretical interpretation or consistency, and relatively little data exist for this important step forming reactive vinylidene H_2CC. We will work with the Stanford group for prompt resolution. This is particularly important because ethylene is the main pyrolysis product of larger hydrocarbon fuels.[7]

Product identity can be as important an issue as the rate constant, although not always recognized, and may also be temperature and pressure dependent. Proper treatment most often relies on quantum calculations of potential energy surface properties, then to be employed in master equation rate calculations. Competitions between chemical activation and recombinations form one example. Reactions where product choice alters the number of radical species or their degree of reactivity are of greatest importance. In the course of this combined evaluation/optimization mechanism development, several such reactions were identified for further needed study. These include H atom yields from the $O + CH_3$ and $CH_2 + O_2$ oxidation reactions, and product branching fractions for the $C_2H_3 + O_2$ reaction.

To illustrate our approach to rate constant and uncertainty evaluation for multiple product reactions, we present an example of results for the pressure dependence of recommended rate constants for $OH + CH_3$ at 1000 K. There are two main product channels, recombination to form methanol (CH_3OH), and a nearly thermoneutral reaction producing $^1CH_2 + H_2O$ (followed by additional reactions). At high pressure all nascent hot methanol is collisionally stabilized and recombination dominates; at low pressure the hot complex decomposes either back to reactants or to methylene product, and the chemical activation step dominates. The evaluated mechanism rate constants for these two paths are shown in Figure 8, based on RRKM rate theory calculations from GRI-Mech done to match high temperature shock tube methanol decomposition data and room temperature $OH + CH_3$ rate constant measurements. Note the clear, expected, pressure-dependent switching in the main products as pressure increases. The

star points in the figure represent recent measurements (both channels) at Stanford[8] and Argonne,[9] which indicate somewhat lower values, and that a factor of 2.5 uncertainty on the low side should be accommodated in the chemical activation rate constant. A theory study,[10] marked T in the figure, significantly underpredicts the rapid rate for the chemical activation pathway.
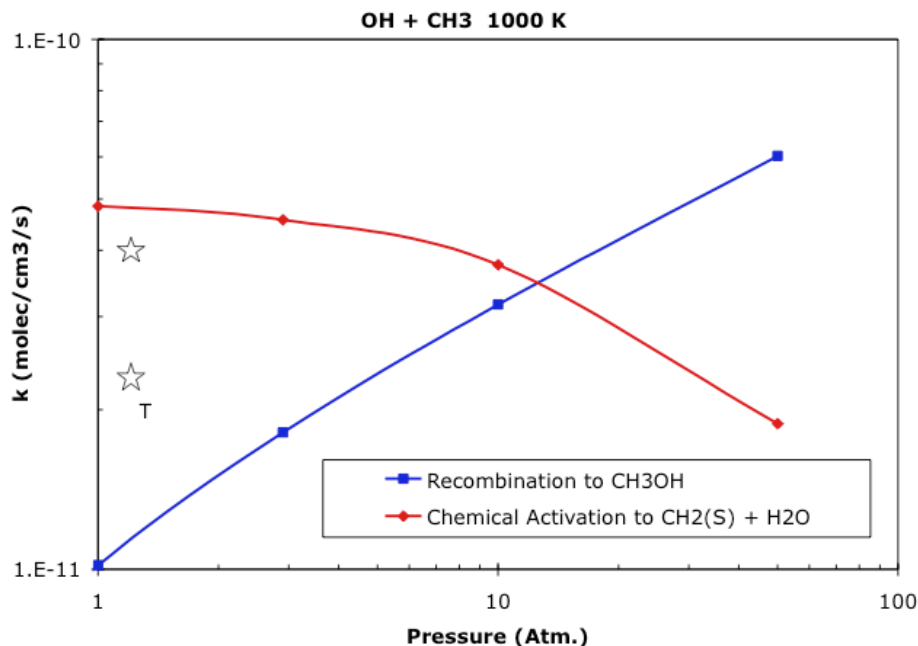

OH + CH3 1000 K

Figure 8. Bimolecular Model Rate Constants for OH + CH$_3$ at 1000 K vs. Pressure for Two Product Channels. Stars and T are experimental and theoretical total rate constant values near 1 atm; see text for details.

Inclusion of more species was also considered. For acetylene oxidation, the adduct C$_2$H$_2$OH has a modestly strong bond, probably should be added, and its kinetics were developed for later inclusion. There may also be some problems accurately simulating very rich kinetics until C3-4 species associated with presooting kinetics are included in later mechanism versions.

We examined adding peroxide kinetics for lower temperature scenarios and provide recommended rates. Methyl hydroperoxide kinetics begin to matter (>30%) for methane ignition below 1000 K. While optimization targets are generally not available and low temperature oxidation is usually insignificantly slow in most scenarios, inclusion of this chemistry is recommended in the future. Ethyl hydroperoxide kinetics has less impact for ethane oxidation and ignition. Small ~25% effects are seen at 900-1100 K, as Glarborg has previously noted.[11] Other more weakly bound species we considered, C$_2$H$_5$O and C$_2$H$_4$OH, can be assumed decomposed and omitted from the mechanism. We also do not include CH$_3$CHOH, and C$_2$H$_3$O$_2$.

We have also developed some lightly-reviewed high temperature kinetics for the oxygenated C2 fuels that do not appear to have any significant impact on the normal hydrocarbon oxidation kinetics. These are ethanol, dimethyl ether(DME), and methyl formate (C$_2$H$_5$OH, CH$_3$OCH$_3$, CH$_3$OCHO), and could be added to the mechanism for these fuels. This is for completeness, with no performance guarantees; for DME all the lower temperature peroxy kinetics were truncated and omitted. Other added species to these mechanisms are CH$_3$OCH$_2$ and CH$_2$OCHO.

In many instances, pressure dependent expressions for reactions had to be adapted from theory/experiment literature for use, and more precise calculation would be useful. The multiple channels and pressure dependent chemical activation steps are becoming more prevalent with larger species and can have more complex dependences that are harder to parameterize. It might be better to treat these with separate interpolatable expressions for specific pressure levels, rather than current older Chemkin formulations.

An initial review was undertaken for species and reactions that must be added to describe C-3 hydrocarbon oxidation. Most useful available inputs come from Curran's Aramco model.[12,13] Key questions include which aldehyde and alcohol intermediates require inclusion, and whether cyclic compounds also need consideration. At this point we face an evaluation task involving at least 16-24 species and 215 reactions. Data is sparse, more so for C-4 species, and greater reliance on theory and analogy to similar reactions is anticipated.

REFERENCES

1. G. W. Faris, A. Markosyan, C. L. Porter, and S. Doshay, "Two-tone frequency-modulation stimulated Rayleigh spectroscopy," Opt. Lett. **39**, 4615-4618 (2014).

2. K. S. Kalogerakis, B. H. Blehm, R. E. Forman, C. Jirauschek, and G. W. Faris, "Stimulated Rayleigh and Brillouin scattering in a supercritical fluid," J. Opt. Soc. Am. B **24**, 2040-2045 (2007).

3. C. Baltes and G. W. Faris, "Frequency domain measurements on turbid media with strong absorption using the PN approximation," Appl. Opt. **48**, 2991-3000 (2009).

4. G. P. Smith, D. M. Golden, M. Frenklach, M., N. W. Moriarty, B. Eiteneer, M. Goldenberg, C. T. Bowman, R. K. Hanson, S. Song, W. C. Gardiner, V. Lissianski, Z. Qin, "GRI-Mech 3.0" from http://combustion.berkeley.edu/gri-mech/.

5. X. Q. You, A. Packard, and M. Frenklach, "Process informatics tools for predictive modeling: Hydrogen combustion," Int. J. Chem. Kinet. **44**, 101-116 (2012).

6. G. L. Pilla, D. F. Davidson, and R. K. Hanson, "Shock tube/laser absorption measurements of ethylene time-histories during ethylene and n-heptane pyrolysis," P. Combust. Inst. **33**, 333-340 (2011); private communication.

7. C. T. Bowman, R. K. Hanson, and H. Wang, "Modeling pyrolysis and oxidation of actual H-C jet fuels - a physics-based hybrid approach," in *MACCCR - Multi-Agency Coordinating Committee for Combustion Research 2014* (NIST, Boulder, Colorado., 2014).

8. V. Vasudevan, R. D. Cook, R. K. Hanson, C. T. Bowman, and D. M. Golden, "High-temperature shock tube study of the reactions CH_3+OH -> products and CH_3OH+Ar -> products," Int. J. Chem. Kinet. **40**, 488-495 (2008).

9. N. K. Srinivasan, M. C. Su, and J. V. Michael, "High-temperature rate constants for CH_3OH+Kr -> products, $OH+CH_3OH$ -> products, $OH+(CH_3)_2CO$ -> $CH_2COCH_3+H_2O$, and $OH+CH_3$ -> CH_2+H_2O," J. Phys. Chem. A **111**, 3951-3958 (2007).

10. A. W. Jasper, S. J. Klippenstein, L. B. Harding, and B. Ruscic, "Kinetics of the reaction of methyl radical with hydroxyl radical and methanol decomposition," J. Phys. Chem. A **111**, 3932-3950 (2007).

11. C. L. Rasmussen, J. G. Jakobsen, and P. Glarborg, "Experimental measurements and kinetic modeling of CH_4/O_2 and $CH_4/C_2H_6/O_2$ conversion at High pressure," Int. J. Chem. Kinet. **40**, 778-807 (2008).

12. W. K. Metcalfe, S. M. Burke, S. S. Ahmed, and H. J. Curran, "A Hierarchical and Comparative Kinetic Modeling Study of C-1 - C-2 Hydrocarbon and Oxygenated Fuels," Int. J. Chem. Kinet. **45**, 638-675 (2013).

13. W. K. Metcalfe, S. Burke, and H. J. Curran, "AramcoMech 1.3," from http://c3.nuigalway.ie/ (2013).

PERSONNEL

The following personnel participated in the research supported by this contract during this project:

- Gregory W. Faris, Program Manager, principal investigator and lead experimentalist
- Gregory P. Smith, Senior Research Chemist, co-principal investigator
- Daniel Matsiev, investigator
- Chia-Pin Pan, investigator
- Sanhita Dixit, investigator
- Paul Gefken, technical advice
- William Olson, technical support
- Robert Bell, technical support
- Tom Lovelace, technical support

PUBLICATIONS

G. W. Faris, A. Markosyan, C. L. Porter, and S. Doshay, "Two-tone frequency-modulation stimulated Rayleigh spectroscopy," Opt. Lett. **39**, 4615-4618 (2014).

PRESENTATIONS

- G. W. Faris "Supercritical Fuel Measurements Using Stimulated Scattering," presented at Multi-Agency Coordination Committee for Combustion Research (MACCCR) meeting, Arlington, VA, September 23-26, 2013

- G. Smith, Y. Tao, H. Wang, E. Dames, "C0-C4 Foundational Fuels Optimized Chemistry," presented at 7th MACCCR Fuels and Combustion Research Review, Boulder CO, Oct. 28, 2014.

INTERACTIONS/TRANSITIONS

- MACCR meeting: Multi-Agency Coordination Committee for Combustion Research (MACCCR) The 6th- Annual Fuel and Combustion Research Review, Arlington Virginia, September 23-26, 2013: Gregory Faris was an attendee and presenter.
- AFOSR/ARO Basic Combustion Research Review Contractors' Meeting, Arlington Virginia, June 2-6, 2014: Gregory Faris and Gregory Smith were attendees and participants.
- MACCR meeting: 7th Multi-Agency Coordination Committee for Combustion Research (MACCCR), Boulder, CO, October 27-30, 2014. Gregory Smith was an attendee and presenter.
- Collaboration with Prof. Hai Wang and Dr. Enoch Dames at Stanford in the kinetics evaluations and optimization for the foundational fuels combustion mechanism. This effort was initially supported by the CEFRC program funded by DOE, in addition to and at present by AFOSR.
- Discussions with Tim Edwards of WPAFB regarding fuels properties.
- Discussions with Tom Bruno of NIST regarding supercritical instrumentation and measurements
- Discussions with Terry Parker of the Colorado School of Mines regarding supercritical experiments.
- Discussions with Robert Kee of the Colorado School of Mines regarding supercritical properties.

INVENTIONS/DISCOVERIES

No invention disclosures or patent applications were filed.

HONORS/AWARDS

Gregory Faris is a recipient of SRI International's Fellow Award for 2014. This is SRI's highest honor for technical achievement. Gregory Smith received this award in 2003.

APPENDIX

G. W. Faris, A. Markosyan, C. L. Porter, and S. Doshay, "Two-tone frequency-modulation stimulated Rayleigh spectroscopy," Opt. Lett. **39**, 4615-4618 (2014).

Two-tone frequency-modulation stimulated Rayleigh spectroscopy

Gregory W. Faris,[1,*] Ashot Markosyan,[2] Christina L. Porter,[3] and Sage Doshay[4]

[1]*Molecular Physics Laboratory, SRI International, 333 Ravenswood Avenue, Menlo Park, California 94025-3493, USA*

[2]*E. L. Ginzton Laboratory, Stanford University, 348 Via Pueblo Mall, Stanford, California 94305-4088, USA*

[3]*Department of Electrical Engineering, Engineering Quadrangle, Olden Street, Princeton, New Jersey 08544, USA*

[4]*Department of Applied Physics, 348 Via Pueblo Mall, Stanford University, Stanford, California 94305-4090, USA*

*Corresponding author: gregory.faris@sri.com

We have demonstrated two-tone frequency-modulation (FM) stimulated Rayleigh spectroscopy. This method can provide high spectral resolution (~1 MHz), excellent pump/probe detuning accuracy, and near-shot-noise-limited signal-to-noise ratios using a single narrowband laser as the master oscillator. Pump/probe detuning and FM sideband generation are produced with an electro-optic modulator. A double-pass two-rod Nd:YAG amplifier provides peak powers near 1 kW for the pump beam. Unlike with two-tone FM absorption spectroscopy, the phase signal is retained for two-tone FM Rayleigh spectroscopy. Measurements confirm that the shape of the phase component of the stimulated thermal Rayleigh peak agrees with theory.   © 2014 Optical Society of America

OCIS codes: (190.5890) Scattering, stimulated; (190.1900) Diagnostic applications of nonlinear optics; (290.5870) Scattering, Rayleigh; (300.6320) Spectroscopy, high-resolution; (300.6420) Spectroscopy, nonlinear.

http://dx.doi.org/10.1364/OL.39.004615

Rayleigh scattering, which is produced by nonpropagating thermal or entropy fluctuations in transparent media, can provide information on thermal diffusion, molecular mass diffusion, density, and other material phenomena [1]. Stimulated Rayleigh scattering methods are generally used to provide strong coherent signals. While early work on stimulated Rayleigh scattering was performed using a single laser [2], better resolution and linearity can be achieved using multibeam (pump-probe) methods. Rayleigh scattering methods that use two pump beams to produce a refractive index grating that diffracts the probe beam include forced Rayleigh scattering [3] and grating methods [4], which detect scattering in the temporal domain, and coherent Rayleigh scattering [5] and phase-coherent Rayleigh scattering with detection in the spectral domain [6]. We are using a stimulated Rayleigh gain spectroscopy configuration, which uses a single pump beam, simplifying alignment. Interference between the pump and probe beams produces a grating that diffracts power from the pump onto the probe beam with detection in the spectral domain [7,8].

Compared with other nonlinear scattering methods, such as stimulated Raman spectroscopy and stimulated Brillouin spectroscopy, stimulated Rayleigh scattering provides much weaker signals when relying on electrostriction for coupling between the optical radiation and the material fluctuations [8–10]. However, signals can be made much larger when there is absorption of the laser light to support light/matter coupling, an approach called stimulated thermal Rayleigh scattering [11], which has the same shape as with electrostrictive coupling, but differs in sign [8–10]. For measurements in liquids, we use a wavelength of 1064 nm, at which wavelength OH and CH overtone or combination bands produce weak absorption, providing relatively strong stimulated thermal Rayleigh scattering [7].

An important challenge for stimulated Rayleigh gain spectroscopy involves the narrow linewidths for Rayleigh scattering, which for a counterpropagating geometry are on the order of 10 MHz [9,10], and even narrower in the supercritical regime [12]. By comparison, the linewidths for the pulsed lasers typically used as the pump laser are larger, constrained by the Fourier-transform limit to around 15 MHz [8,13]. Narrow linewidths can be achieved using continuous-wave (CW) lasers for the pump beam [6,14,15], but at the expense of weaker signals. In addition, when using separate pump and probe lasers, maintaining a stable pump/probe detuning may require active stabilization or heterodyne calibration [8,15].

In this Letter, we apply two-tone FM methods to measurement of stimulated Rayleigh scattering. FM spectroscopy is a very sensitive method, typically applied to optical absorption measurements [16]. Radio frequency (RF) phase-modulation (PM) is applied to a laser, producing FM sidebands with no amplitude modulation. When interaction with a sample produces absorption or phase shifts between the sidebands, the resulting imbalance produces amplitude modulation at the modulation frequency. Because laser noise is typically quite low at RF, this provides a sensitive detection method. To achieve both large frequency shifts for absorption measurements while keeping the detection bandwidth low, a modified method has been developed using two modulation frequencies, called two-tone FM spectroscopy [17]. Single-tone FM methods have been applied to Brillouin scattering using separate pump and probe lasers, but FM methods have not been applied to Rayleigh scattering. We demonstrate two-tone FM methods applied to stimulated thermal Rayleigh scattering that allows use of a single master oscillator. The frequencies for the pump and probe lasers are defined by RF frequency shifting, providing exceptionally accurate pump/probe detuning without active stabilization. We achieve a stronger stimulated scattering gain by pulse amplifying part of the master oscillator. Pulse amplification allows much
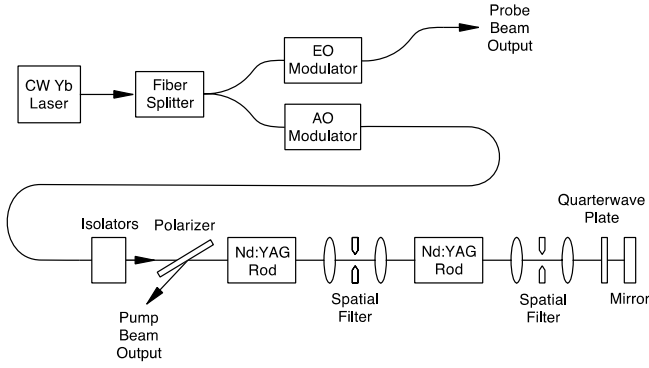
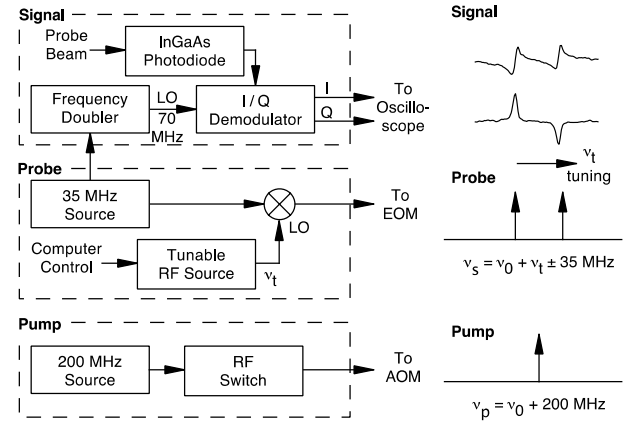Fig. 1. Optical arrangements for producing probe and pump beams.

Fig. 2. Electronics (left) and frequency content (right) for signal detection, probe, and pump (from top to bottom). For clarity, electronic filters and amplifiers are not shown. The frequencies of the master oscillator, pump, and probe (Stokes) beams are denoted as ν_0, ν_p, and ν_s, respectively. LO refers to the RF local oscillator used for the mixing steps.

longer pulse widths than using Q-switched lasers, enabling high-resolution measurement of the Rayleigh peak ($\sim$1 MHz linewidth if Fourier-transform limited).

The optical system for our experiments is shown in Fig. 1. The master oscillator for both the pump and probe beams is a narrowband fiber laser (NP Photonics model RFLS-25-1-1064.175), producing 54 mW at 1064 nm. A fiber beam splitter delivers 30% of the power to the probe beam path and 70% to the pump beam path. The probe beam passes through a fiber-coupled electro-optic modulator (EOM), in this case a Photline model NIR-MPX-LN-10-P-P that provides both the probe frequency tuning and the FM sidebands. The pump beam passes through a fiber-coupled acousto-optic modulator (AOM), in this case a Brimrose model IPF-200-20-1064-2FP that upshifts the pump frequency by 200 MHz. The AOM serves two roles. First, because of the 200 MHz frequency shift in the AOM, the degeneracy of the EOM sidebands relative to the master oscillator frequency is broken. Without this pump frequency shift, the pump would create stimulated scattering with both upper and lower sidebands of the EOM simultaneously, and interference between the two sidebands would produce undesirable variation in the signal. Second, we pulse the RF power to the AOM with an RF switch, allowing adjustment of the pump beam pulse width. Typical pulse widths are 1 μs. After the AOM, the pump beam passes a fiber collimator to free space and then goes through Faraday isolators to prevent feedback into the master oscillator. The pump beam is subsequently amplified to peak powers of roughly 1 kW by double-passing two lamp-pumped Nd:YAG rods (Quantel model SF51107) operating at 10 Hz. The polarized input beam passes through a polarizer and the two Nd:YAG rods, with two spatial filters to reduce parasitic amplified spontaneous emission. A quarter-wave plate and mirror at the far end of the amplifier rods retroreflects the beam while rotating the polarization by $\pi/2$ so that the polarizer redirects the retroreflected beam to the output path. The pump beam then passes a high power Faraday isolator to prevent feedback from the experiment into the pulsed amplifier. The pump and probe beams are focused with long focal lengths ($\sim$2 m) into the measurement cell in a counterpropagating geometry similar to previous experiments [7,8,12].

The electronics for tuning, modulation, and detection are shown in Fig. 2. For the pump beam (bottom of Fig. 2), a 200 MHz RF source is amplitude modulated by the RF

switch to produce a pulse, which is amplified and sent to the AOM. For the probe beam, an RF source with frequency ν_0 tuned by computer control, is mixed with a 35 MHz source to produce two sidebands 70 MHz apart (the center frequency is suppressed in the mixer). These sidebands are amplified and sent to the EOM. Stimulated Rayleigh scattering resonances are found when either sideband is near the pump frequency, i.e., when the tunable RF frequency ν_t is equal to 200 ± 35 or 165 and 235 MHz. A typical measurement scans ν_t from 100 to 300 MHz.

Two-tone modulation produces several pairs of frequencies separated by the detection frequency (70 MHz), with the most prominent ones centered at $\nu_0 + \nu_t$, $\nu_0 - \nu_t$, and ν_0, where ν_0 is the master oscillator frequency. We use the upshifted sideband pair at $\nu_0 + \nu_t$ for these experiments. Previous two-tone FM spectroscopy has been performed on broad absorption features and both sidebands interact with the sample simultaneously. In contrast, for the narrow linewidths of Rayleigh scattering, only a single frequency in the sideband pair interacts with the sample at a time, resulting in spectra similar in appearance to single-tone FM signals. The two-tone FM absorption spectroscopy analysis of Janik et $al.$ [17] for dual sideband interaction may be extended to perturbation of a single sideband. In this case, the resulting two-tone intensity signal $I(\Omega t)$ for $\nu_0 + \nu_t$ at the FM pair separation frequency, Ω, (70 MHz for our experiment) and the sample interaction described by $\exp(-\delta_j - i\phi_j)$ will be

$$I(\Omega t) = -(\delta_{+1} + \delta_{-1})\cos(\Omega t) - (\phi_{+1} - \phi_{-1})\sin(\Omega t), \quad (1)$$

where δ and ϕ are the amplitude attenuation and phase shift from the sample and $j = +1$ and -1 denote the upper and lower sidebands, respectively. Thus, unlike two-tone absorption spectroscopy, which provides only gain/loss measurements, two-tone FM Rayleigh scattering provides both gain/loss and phase terms in quadrature. As is typical for FM spectroscopy, Eq. (1) shows that the single-sideband signal at the sideband difference

frequency Ω is zero unless a sample perturbation δ_j or ϕ_j is present. Typical gain/loss is 10^{-3} of the probe beam.

The detection electronics are shown in the top of Fig. 2. The 70 MHz FM signal is detected using an InGaAs photodiode, bandpass filtered, amplified, and passed to an I/Q (in-phase and quadrature) demodulator. At 70 MHz, the noise on the probe laser is near shot-noise limited. The 70 MHz RF reference frequency (local oscillator) for the I/Q demodulator is produced by frequency doubling a portion of the output of the same 35 MHz source that produces the sidebands, providing phase coherence between the FM signal and the RF reference frequency. The two outputs of the I/Q demodulator are low pass filtered and captured in two channels of a digital oscilloscope. A LabVIEW program controls scanning the RF frequency and storing the stimulated scattering signals.

From Eq. (1), both gain/loss and phase changes are present in the two-tone FM Rayleigh signal. The lineshapes of the gain/loss and phase shift on the probe beam for stimulated thermal Rayleigh scattering are described by the imaginary and real parts of the nonlinear susceptibility $\chi(\Delta\omega)$, which is given by [10,11]

$$\chi_{\text{STRS}}^{(3)}(\Delta\omega) = K \frac{-1 - i(2\Delta\omega/\Gamma_R)}{1 + (2\Delta\omega/\Gamma_R)^2}, \qquad (2)$$

where $\Delta\omega = 2\pi(\nu_p - \nu_s)$ is the pump/probe detuning as an angular frequency, K is a constant that depends on the pump frequency and the sample material properties, and Γ_R is the Rayleigh linewidth as an angular frequency. The laser linewidth contribution to the Rayleigh lineshape is very small for our experiment.

When the phase between the EOM and I/Q demodulator is varied, different linear combinations of the real and imaginary parts of the complex scattering lineshape appear in the I and Q channels. The variation in the FM stimulated Rayleigh scattering signal in hexane as a function of the RF reference frequency phase is shown in Fig. 3, which covers a full 2π phase change. Note that there are two peaks, one at 165 MHz and one at 235 MHz, corresponding to the cases in which the upper and lower FM sidebands are resonant with the Rayleigh gain signal. As the phase changes, each Rayleigh line gradually changes shape from purely antisymmetric (gain/loss) to purely symmetric (phase shift) and then repeats each shape with the opposite sign. The two peaks in Fig. 3 show the expected relationship from Eq. (1): the antisymmetric (gain/loss or δ) features have the same sign for the two sidebands, while the symmetric (phase change or ϕ) features are opposite in sign.

The I/Q modulator detects the signal for two RF phases simultaneously. An I/Q signal pair for stimulated Rayleigh scattering is shown as the dots in Fig. 4. Note that each scan measures the same peak four ways: there is an in phase and a quadrature measurement for both $\nu_t = 165$ and 235 MHz. We have selected the RF reference phase to produce the antisymmetric gain/loss peaks in the I channel (the upper set of points in Fig. 4; this peak shape is well known from prior stimulated thermal gain spectroscopy experiments [7]). The Q channel peaks (bottom points in Fig. 4) correspond to the phase-only changes for stimulated Rayleigh scattering that have not been
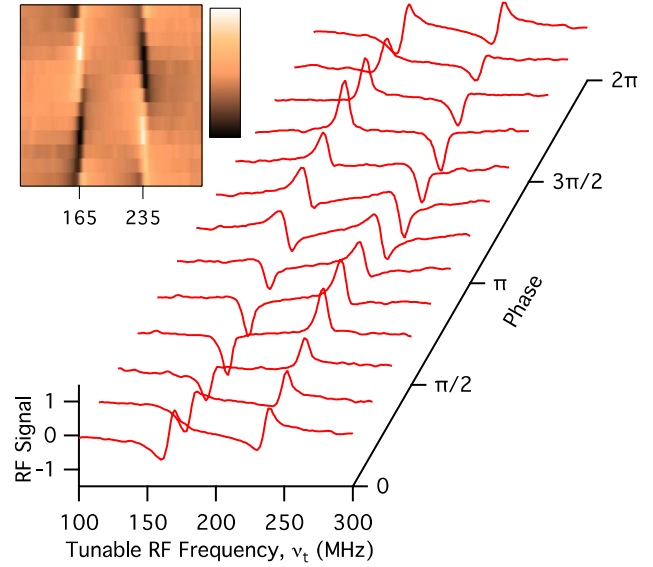

Fig. 3. Variation in experimental two-tone FM stimulated Rayleigh spectra in hexane as a function of delay between the probe and the reference signal to the I/Q demodulator. The waterfall graph is reproduced as an image inset at the upper right.

observed previously with stimulated Rayleigh gain spectroscopy, although a similar complex pair of peaks have been observed using phase-coherent Rayleigh scattering [6].

The results from fitting Eq. (2) to experimental points are shown as the solid lines in Fig. 4, where Γ_R and K are used as fitting parameters. The experimental measurements have the expected relationships between the gain or loss and phase shift of Eq. (2), with the maximum of the symmetric phase shift profile twice as large as the maximum of the antisymmetric gain/loss peak. Performing such fits on multiple Rayleigh peaks yields a Rayleigh
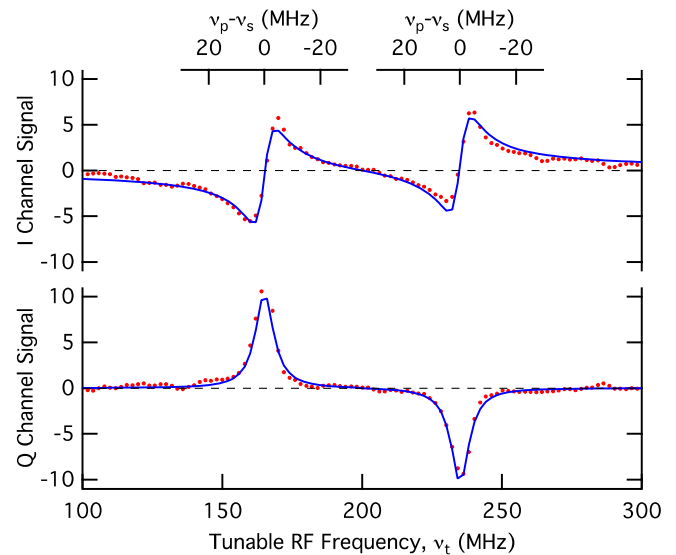

Fig. 4. I and Q channels for two-tone FM stimulated Rayleigh scattering in hexane. There are replicate peaks centered at 165 and 235 MHz. The upper axis (pump/probe detuning) and lower axis (tunable RF frequency) apply to both traces.
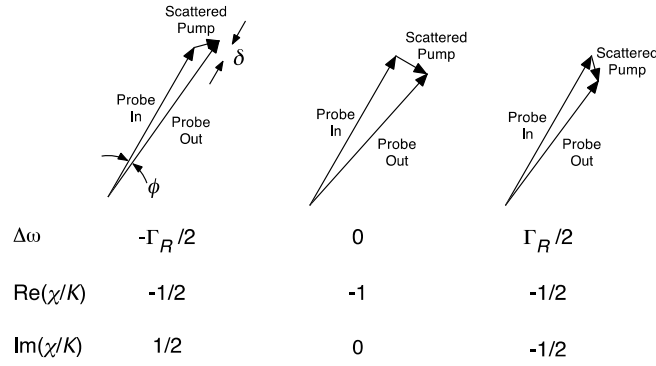
Fig. 5. Phasor diagrams (top) show gain/loss (δ) and phase shift (ϕ) for the output probe beam for different amounts of detuning $\Delta\omega$. The relative gain/loss ($\mathrm{Re}(\chi/K)$ and phase shift $\mathrm{Im}(\chi/K)$ values are listed under the phasor diagrams.

linewidth $\Gamma_R/2\pi = 7 \pm 1$ MHz, in agreement with theory [7].

Note that the gain/loss lineshape at the top of Fig. 4 has an antisymmetric shape (often called "dispersive," although here this is an absorptive feature) while the phase shift lineshape at the bottom of Fig. 4 has a symmetric profile (sometimes called "absorptive," although here this is a dispersive feature). This situation is the opposite of that found in prior experiments on FM spectroscopy using absorption or Brillouin scattering, which have a symmetric ("absorptive") lineshape for a gain or loss signal and an antisymmetric ("dispersive") lineshape for a phase signal [15,16]. The source of the unusual behavior for the stimulated Rayleigh scattering can be understood from the underlying scattering process.

The scattered pump light that forms the stimulated Rayleigh gain signal is automatically phase-matched with the probe, i.e., the two light fields have the same wave vector, $\mathbf{k}$. This phase-matched condition is assured because the grating that scatters the pump in the probe direction is produced by interference between the pump and probe beams. As a result, the grating satisfies a Bragg condition to scatter the pump collinearly with the probe, and the Doppler shift resulting from the moving grating (the grating moves with nonzero detuning) shifts the pump beam frequency by the necessary amount to match the probe frequency. Although the scattered pump and probe have the same wave vectors, the phase of the two beams is not the same.

How this phase shift for the scattered pump produces the Rayleigh peak shapes can be understood from Fig. 5, which shows the output probe beam electric field as a vector sum of the electric fields of the input probe beam and the scattered pump. When there is no detuning ($\Delta\omega = 0$), the scattered pump light is $\pi/2$ out of phase with the probe beam. This leads to a maximum phase shift and no change in the magnitude of the output electric field for the probe beam when $\Delta\omega = 0$, as seen in Fig. 5. In the detuned case, the magnitude of the scattered pump decreases and the scattered pump phase shifts

away from $\pi/2$. These positive and negative detunings lead to gain and loss, respectively, for the magnitude of the output probe electric field, and a reduction in the phase change as seen in Fig. 5.

Two-tone stimulated scattering has multiple advantages for Rayleigh spectroscopy, including high frequency resolution and precision with a pulsed laser (1 MHz), near-shot-noise-limited signal-to-noise ratios, and measurement of both absorptive and dispersive peaks. The technique should prove valuable for studies in supercritical fluids and can be extended to Brillouin spectroscopy as well.

References

1. H. J. Eichler, P. Günter, and D. W. Pohl, *Laser-Induced Dynamic Gratings* (Springer-Verlag, 1986).
2. D. H. Rank, C. W. Cho, N. D. Foltz, and T. A. Wiggins, Phys. Rev. Lett. **19**, 828 (1967).
3. D. W. Pohl, S. E. Schwarz, and V. Irniger, Phys. Rev. Lett. **31**, 32 (1973).
4. H. Eichler, G. Salje, and H. Stahl, J. Appl. Phys. **44**, 5383 (1973).
5. J. H. Grinstead and P. F. Barker, Phys. Rev. Lett. **85**, 1222 (2000).
6. S. Takagi and H. Tanaka, Rev. Sci. Instrum. **73**, 3337 (2002).
7. G. W. Faris, M. Gerken, C. Jirauschek, D. Hogan, and Y. Chen, Opt. Lett. **26**, 1894 (2001).
8. C. Jirauschek, E. M. Jeffrey, and G. W. Faris, Phys. Rev. Lett. **87**, 233902 (2001).
9. W. Kaiser and M. Maier, in *Laser Handbook*, F. T. Arecchi and E. O. Schulz-Dubois, eds. (North-Holland, 1972), Vol. **2**, pp. 1077–1150.
10. R. W. Boyd, in *Nonlinear Optics* (Academic/Elsevier, 2008), pp. 429–471.
11. R. M. Herman and M. A. Gray, Phys. Rev. Lett. **19**, 824 (1967).
12. K. S. Kalogerakis, B. H. Blehm, R. E. Forman, C. Jirauschek, and G. W. Faris, J. Opt. Soc. Am. B **24**, 2040 (2007).
13. G. W. Faris, M. J. Dyer, and W. K. Bischel, Opt. Lett. **19**, 1529 (1994).
14. K. Ratanaphruks, W. T. Grubbs, and R. A. MacPhail, Chem. Phys. Lett. **182**, 371 (1991).
15. T. Sonehara, Y. Konno, H. Kaminaga, S. Saikan, and S. Ohno, J. Opt. Soc. Am. B **24**, 1193 (2007).
16. G. C. Bjorklund, Opt. Lett. **5**, 15 (1980).
17. G. R. Janik, C. B. Carlisle, and T. F. Gallagher, J. Opt. Soc. Am. B **3**, 1070 (1986).

1.

1. Report Type

Final Report

Primary Contact E-mail
Contact email if there is a problem with the report.

gregory.faris@sri.com

Primary Contact Phone Number
Contact phone number if there is a problem with the report

650-859-4131

Organization / Institution name

SRI International

Grant/Contract Title
The full title of the funded effort.

Research in Supercritical Fuel Properties and Combustion Modeling

Grant/Contract Number
AFOSR assigned control number. It must begin with "FA9550" or "F49620" or "FA2386".

FA9550-13-1-0177

Principal Investigator Name
The full name of the principal investigator on the grant or contract.

Gregory W. Faris

Program Manager
The AFOSR Program Manager currently assigned to the award

Chiping Li

Reporting Period Start Date

06/15/2013

Reporting Period End Date

06/14/2015

Abstract

The objectives of this research are to develop stimulated scattering as a diagnostic for supercritical fluids, and to evaluate reaction kinetics inputs involving 2-4 carbon atom species for combustion modeling and optimization. On the stimulated scattering task, we have tested new methods for rapidly scanning stimulated scattering measurements, achieving a factor of 1,000 improvement in the single shot spectroscopy measurement rate; developed models for two-tone stimulated Rayleigh scattering signals; published a paper on our new two-tone stimulated scattering method, implemented frequency domain measurements for refractive index measurements, and tested our supercritical cell. On the reaction kinetics task, review and evaluation of reactions, rate parameters, and uncertainties for combustion of 2-carbon species for the initial foundational fuels mechanism optimization was completed. We identified reactions needing further study and C-2 and C-3 species to add to the mechanism.

Distribution Statement
This is block 12 on the SF298 form.

Distribution A - Approved for Public Release

Explanation for Distribution Statement
If this is not approved for public release, please provide a short explanation. E.g., contains proprietary information.

DISTRIBUTION A: Distribution approved for public release.

SF298 Form

Please attach your **SF298** form. A blank SF298 can be found **here**. Please do not password protect or secure the PDF
The maximum file size for an SF298 is 50MB.

   P21929 AFOSR SF298.pdf

Upload the Report Document. File must be a PDF. Please do not password protect or secure the PDF . The maximum file size for the Report Document is 50MB.

   P21929 AFOSR Final v9.pdf

Upload a Report Document, if any. The maximum file size for the Report Document is 50MB.

Archival Publications (published) during reporting period:

G. W. Faris, A. Markosyan, C. L. Porter, and S. Doshay, "Two-tone frequency- modulation stimulated Rayleigh spectroscopy," Opt. Lett. 39, 4615-4618 (2014).

Changes in research objectives (if any):

None.

Change in AFOSR Program Manager, if any:

None.

Extensions granted or milestones slipped, if any:

None.

AFOSR LRIR Number

LRIR Title

Reporting Period

Laboratory Task Manager

Program Officer

Research Objectives

Technical Summary

Funding Summary by Cost Category (by FY, $K)

	Starting FY	FY+1	FY+2
Salary			
Equipment/Facilities			
Supplies			
Total			

Report Document

Report Document - Text Analysis

Report Document - Text Analysis

Appendix Documents

2. Thank You

E-mail user

Sep 14, 2015 20:44:30 Success: Email Sent to: gregory.faris@sri.com